Control of an Interior PM Synchronous Machine for Operating as Integrated Starter-Generator

VASILE HORGA, DORIN LUCACHE, MARCEL RĂȚOI,
ALECSANDRU SIMION, MIHAI ALBU
Faculty of Electrical Engineering
”Gh. Asachi” Technical University of Iaşi
53 D. Mangeron Blvd., Iaşi, 700050
ROMANIA
http://www.ee.tuiasi.ro

Abstract: - The interior permanent magnet (IPM) synchronous machines have several desirable features for automotive applications. A combined starter-generator is an opportunity for new electrical and behavioral features and higher voltages in automobiles. The paper presents a control structure of an IPM synchronous machine dedicated to act as integrated starter-generator. Test results for both cranking and generation are shown and analyzed.

Key-Words: - integrated starter-generator**,** interior permanent magnet, flux weakening

1 Introduction

Integrated starter generator (ISG) uses one machine to replace conventional starter and alternator onboard vehicles and provides greater electrical generation capacity and improves the fuel economy and emissions. The ISG is coupled to the combustion engine either directly or by a belt.

Nowadays much of the work was done to get the best substitute of the old Lundell alternator. Unlike the machine in pure electric vehicle, the ISG machine has to enable the charging of the battery and to operate electric loads with nearly constant voltage at the speed range corresponding to the engine speed from idle 600rpm to redline 6000rpm.

A special attention was paid to find the existing electric machines that meet the specifications on cranking torque, driving power and speed range at the same time. The continuous cost reduction of magnetic materials with high energy density and coercitivity led to consider the permanent magnet (PM) synchronous machines as high attractive candidates both in automotive, tools machines and residential drive applications.

The IPM motors due to their saliency develop supplementary reluctance torque and thus present a higher torque capability than the surface-mounted permanent magnet synchronous machine (SPMSM). This is why we chose the IPM synchronous machine (IPMSM) to play the role of an ISG.

Because of its geometry, IPMSM has a robust rotor construction, a rotor saliency and the low effective airgap. These features permit control of the machine not only in the constant torque region but also in the constant power region up to a high speed. To get this, some various control algorithms for flux weakening have been published mainly in the last two decades [1]..[7].

The main requirements of the ISG control are to ensure the necessary high torque as starter and the constant output voltage, irrespective of the input speed and load, as generator.

In this paper, the IPMSM play the role of an ISG and is controlled in order to achieve rapid starting and appropriate voltage supply on the DC bus. The control algorithm is a combination of some techniques found in the literature and is based on the maximum torque-per-ampere strategy (minimum copper loss). A prototype system shown in Fig.1 was tested in order to confirm the control algorithms and dSPACE based experimental results are presented and discussed.

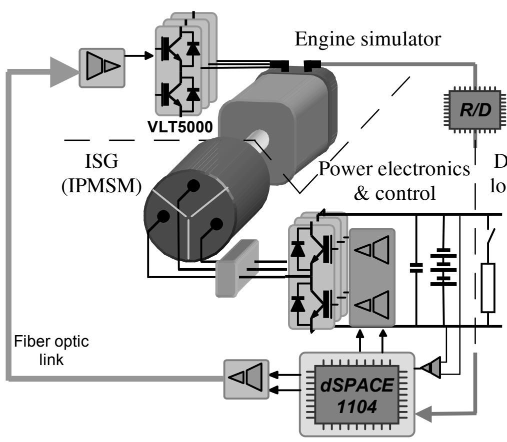

Fig.1 Experimental setup

2 Mathematical model

In the *d-q* axis synchronous frame, the dynamic equations of the IPMSM can be expressed as:

$$\begin{cases} u_{sd} = R_s i_{sd} + L_d \dfrac{di_{sd}}{dt} - \omega_e L_q i_{sq} \\ u_{sq} = R_s i_{sq} + L_q \dfrac{di_{sq}}{dt} + \omega_e L_d i_{sd} + \omega_e \psi_m \end{cases} \quad (1)$$

Symbols u and i denote voltage and current, ψ_m the flux linkage of the permanent magnets in the d-axis rotor, L_d is the d-axis self-inductance, L_q is the q-axis self-inductance, ω_e is the electrical speed, respectively, and index s denotes parameters and variables associated with stator.

The developed electromagnetic torque t_e in terms of stator currents is expressed as:

$$t_e = p\left[\psi_m i_{sq} - \left(L_q - L_d\right) i_{sd} i_{sq}\right] \quad (2)$$

where p denotes the number of pole pairs. This has two components: the alignment torque produced by the flux linkage and the reluctance torque produced by the saliency. It is desirable that the reluctance torque should be properly utilized in order to increase the whole efficiency of the IPMSM drives.

At the low speed, the back-electromotive force is small and so there is enough voltage to control the current to generate the torque. As the rotor speed increases, the marginal voltage to control the current is decreased and the torque becomes highly distorted so the flux weakening method should be applied [1]. The extension range of the speed is solely limited by the structure and the parameters of the motors under the given condition of voltage and current limitation.

The maximum voltage $U_{s\,max}$ that the inverter can supply the machine is limited by DC link voltage and PWM strategy. When the voltage space vector strategy is used, $U_{s\,max} = U_{DC} / \sqrt{3}$. Also the maximum current $I_{s\,max}$ is determined by the inverter current rating and machine thermal rating.

So, the imposed limits for the motor's voltage and current are:

$$\begin{cases} u_{sd}^2 + u_{sq}^2 \le U_{s\,max}^2 \\ i_{sd}^2 + i_{sq}^2 \le I_{s\,max}^2 \end{cases} \quad (3)$$

Neglecting the stator resistance (when speed increases the term ω_e becomes more important), from (1) the steady-state voltage limit equation yields:

$$\left(i_{sd} + \frac{\psi_m}{L_d}\right)^2 \left(\frac{L_d}{L_q}\right)^2 + \left(i_{sq}\right)^2 \le \left(\frac{U_{s\,max}}{\omega_e L_q}\right)^2 \quad (4)$$

From (3) and (4) it can be seen that the current limit equation determines a circle with a radius of $I_{s\,max}$, while the voltage limit equation determines a series of nested ellipses (for the IPMSM, $L_q > L_d$). Fig.2 shows the current-limit circle and the voltage-limit ellipses in the i_{sd}-i_{sq} plane.

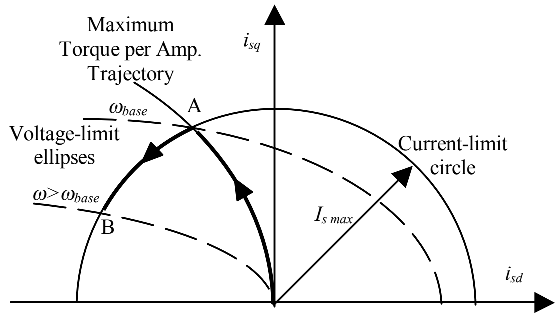

Fig.2 Current-limit circle and voltage-limit ellipses in the i_{sd}-i_{sq} plane

The voltage-limit ellipse decreases as the speed increases. At a so-called base speed ω_{base}, the maximum torque point A is on the cross point of maximum torque-per-current trajectory and current-limit circle. When the IPMSM is operated from the start up to the base speed in the constant torque region, the voltage-limit ellipse exceeds the maximum current boundary and no voltage limitation needs to be considered in this situation.

But beyond the base speed, the IPMSM cannot be operated without flux-weakening control and so, to extend the speed range, a proper demagnetizing current has to be applied depending on the operating speed. The current vector trajectory will move along the boundary of the current-limit circle (from A to B in Fig.2) as rotor speed increases.

Without a proper flux weakening at higher speed, the current regulators would be saturated and lose their controllability. Since the onset of current regulator saturation varies according to the load conditions and the machine parameters, the beginning point of the flux weakening should be varied. The late starting of the flux weakening may result in undesired torque drop, but the early starting deteriorates the acceleration performance [2].

3 The control scheme

As opposed to SPMSM, the i_d=0 control method is not suitable for the IPMSM because the reluctance torque is not produced even if this kind of machine has a saliency.

At low speeds, because the absence of voltage limitation, the current vector might be controlled to fully use reluctance torque in order to maximize the machine efficiency. Typically, it is chosen to maximize the torque per amper ratio by controlling the current vector in order to have an optimum inclination versus q-axis. To get the maximum torque control, the inclination angle γ of the current vector (Fig.3) depends on the load conditions, taking values between 0 and 45° [3].

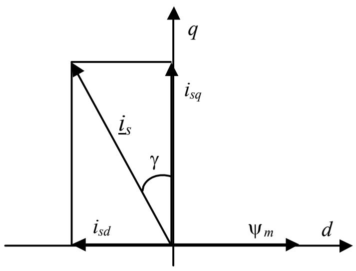

Fig.3 Current phasor diagram in the *d-q* frame

The maximum torque-per-ampere strategy seeks to get a certain torque with the smallest possible stator current amplitude (so with minimum copper loss). Because $i_{sd} = -i_s \sin\gamma$ and $i_{sq} = i_s \cos\gamma$, where $i_s = |\underline{i_s}|$, (2) becomes:

$$t_e = p\left[\psi_m i_s \cos\gamma + \frac{1}{2}\left(L_q - L_d\right)i_s^2 \sin 2\gamma\right] \quad (5)$$

and imposing the condition :

$$dt_e / d\gamma = 0 \quad (6)$$

the relation between i_{sd} and i_{sq} for the maxim torque per amper control is derived as

$$i_{sd} = \frac{\psi_m}{2\left(L_q - L_d\right)} - \sqrt{\frac{\psi_m^2}{4\left(L_q - L_d\right)^2} + i_{sq}^2} \quad (7)$$

This relation is shown as the maximum torque-per-ampere trajectory in Fig.2.

Above the base speed, the normal operation is possible only applying the flux weakening and the maximum torque is obtained when the drive operates in the voltage and current limits. The flux weakening control of PM synchronous machines is conducted by injecting the *d*-axis current i_{sd} negatively, which is different from induction machine where the flux is weakened by decreasing the *d*-axis current.

However, another relation between i_{sd} and i_{sq} could be established and so the control in the constant torque region and constant power region is based on different equations. Some authors, as [3], proposed an algorithm for the control mode transition, but all kind of transitions can lead to instability. The authors of [1] proposed another method by adjusting the *d*-axis current command depending as well as the bounds of the maximum *q*-axis current of the speed controller in the following manner: the *d*-axis current is fixed as a transient which is initiated such that the *q*-axis current bound can be gradually adjusted by a PI controller. The corresponding *q*-axis bound is calculated simultaneously as the PI controller adjusts the *d*-axis current, but it is found that under transient conditions cannot follow the true bounds instantaneously. Other authors like [4] pointed out that the PI controller should be replaced by an integral (I) controller to either ensure the drive stability or simplify the controller design. In order to eliminate the gradual adjustment by feedback mechanisms so as to achieve faster response and better stability [5] proposed o new flux-weakening control method based on a closed-form solution of the available maximum torque.

The proposed control scheme in Fig.4 is a combination of the previous discussed techniques. The *d*–axis and *q*-axis currents cannot be controlled independently by u_{sd} and u_{sq} because of the cross-coupling effects (the terms $\omega_e L_q i_{sq}$ and $\omega_e L_d i_{sd}$ in (1)) that are dominant for IPMSM due to relatively large inductances and increase as the speed increase. The cross-coupling effects are usually canceled by the feedforward compensation [3].

Two PI controllers, implemented in the synchronous reference frame, are used for the current control, followed by a decoupling circuit. In the constant power operation, a closed-loop voltage control is used to ensure an automatically onset of the accurate flux-weakening operation, depending on the load condition and machine parameters. Flux weakening mode is entered when the error

$$\varepsilon = u_{s\,max}^2 - \left(u_{sd}^2 + u_{sq}^2\right) < 0 \quad (8)$$

becomes negative. This error, passing through a low-pass filter (LPF) and regulated by an I controller, lead to the *d*-axis current increases toward the negative direction to prevent saturation of the current regulators. The I controller output is limited (to avoid irreversible demagnetization) so that the *d*-axis current to be between 0 and the minimal allowable $i_{sd}^* = -I_{sd\,max}$.

The magnitude of the injected stator current i_s can be expressed as

$$i_s = \sqrt{i_{sd}^2 + i_{sq}^2} \quad (9)$$

and taking into account (2), the *d-q* axis components of the current vector that ensures the maximum torque-per-ampere yields

$$i_{sq} = sign\left(i_s\right) \cdot \sqrt{i_s^2 - i_{sd}^2} \quad (10)$$

where

$$i_{sd} = \frac{\psi_m - \sqrt{\psi_m^2 + 8\left(L_q - L_d\right)^2 i_s^2}}{4\left(L_q - L_d\right)} \quad (11)$$

The last equation is equivalent with (7) but expressing the *d*-axis current as a function of i_s, taking into account (9).

Thus, when the *d*-axis current is increased with respect to the voltage limit, the *q*-axis current is

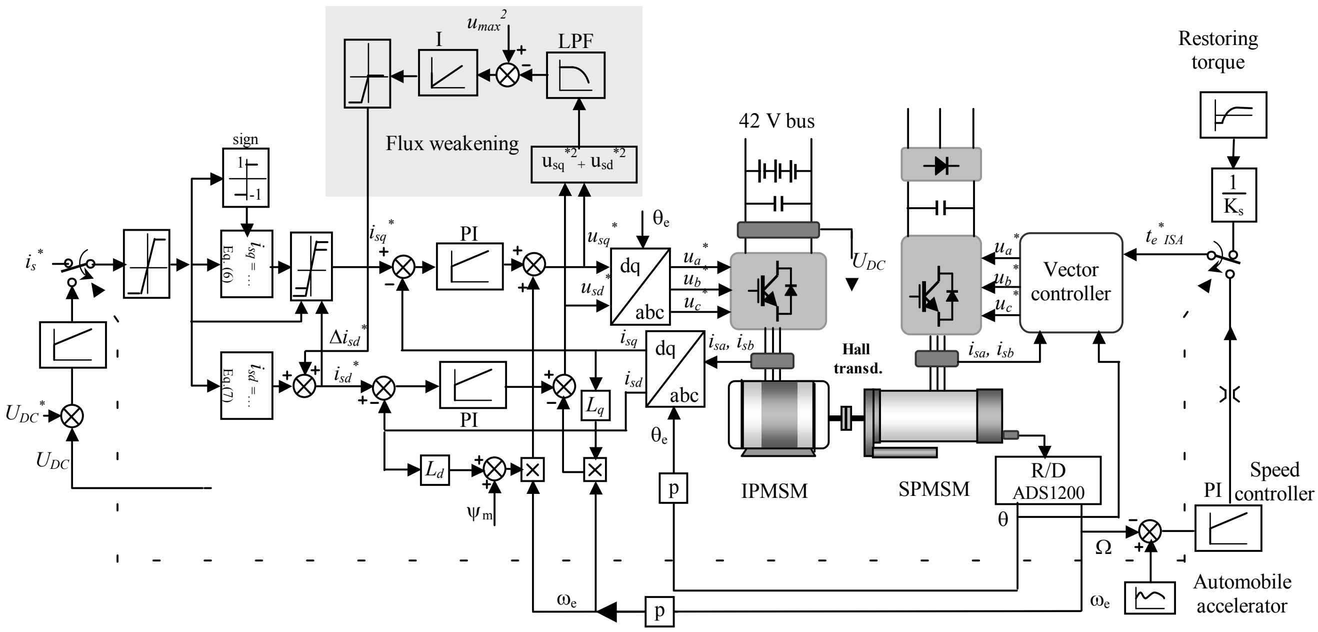

Fig.4 Implemented control system

depressed in order to ensure the current limit condition. Moreover, a saturation block with adaptive limits take into account the flux weakening command Δi_{sd}^{*} and forces ones more the operating point to not exceed the current-limit circle. In this way the current regulators regain the ability of regulating the *d*-axis and *q*-axis currents and the maximum torque-per-ampere is produced at the crossing point between the current limit circle and voltage limit ellipse, in the constant power region.

Because this scheme utilizes for flux weakening the output voltage of the PI current regulators and the outer voltage-regulating loop instead of the IPMSM model, it becomes robust and insensitive to load conditions and load parameters.

4 Experimental results

In this paper a commercial IPMSM, operating at low voltage and high currents, was used (rated parameters in Table 1). This is mechanical coupled (Fig.5) to an internal combustion engine simulator that consists in a SPMSM (1.9 kW, 330V, 4.4A and 4000rpm). The speed of the engine simulator can be varied in closed loop by means of its own inverter. Though the obtained speed characteristics may be different from a real engine, and the power ratio between ISG and engine simulator is not proper, this experimental setup allows testing the validity of the proposed control algorithms successfully.

The PWM converter connected to ISG is a standard three-phase bridge that is capable of bi-directional power flow. In the ISG motoring mode this converter acts as an inverter and in the generating mode it acts as a boosting rectifier.

To control the whole ISG system, a dSPACE 1104 board and ControlDesk software is being used. This board contains all the peripherals and resources necessary to control simultaneously both the engine and ISG. The speed information comes from the resolver included in the SPMSM and is digitalized with an ADS1200 resolver to digital converter. For the currents and the voltages measure the Hall transducers are used.

The external lead-acid battery pack has a double

Table1 IPM synchronous machine characteristics

Rated power [kW]	4
Peak current constraint [A]	160
Number of phases	3
Number of poles	12
R_s [mΩ]	21
L_d [mH]	0.076
L_q [mH]	0.12
ψ_m [Wb]	0.009
Rated speed [rpm]	2000
Rated voltage [V]	11

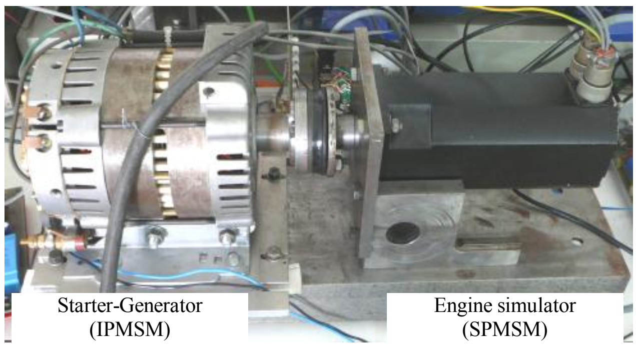

Fig.5 View of the test bench

role: provide the energy necessary in the ISG motoring mode and store the energy produced in the generating mode. A capacitive filter is connected to the DC line.

The following figures present the experimental results for a time interval of two seconds. In the first moments, during 0.28 sec, the engine is cranked by the ISG from 0 up to 600rpm. As motor, the ISG takes a large current from batteries to generate the necessary cranking torque. Once the speed gets 600rpm, the engine control system switched on the speed loop, producing acceleration up to the reference cruise speed (in our case 1200rpm).

At this new speed level, the ISG control system changes from the motoring to generating regime. In the generating regime, the PWM inverter boosts up to about 38V on the DC link, charging the batteries pack with a low current (approx. 1.2A) as in Fig.7.

A special attention was paid to handle the non-sinusoidal currents produced by the IPMSM due to

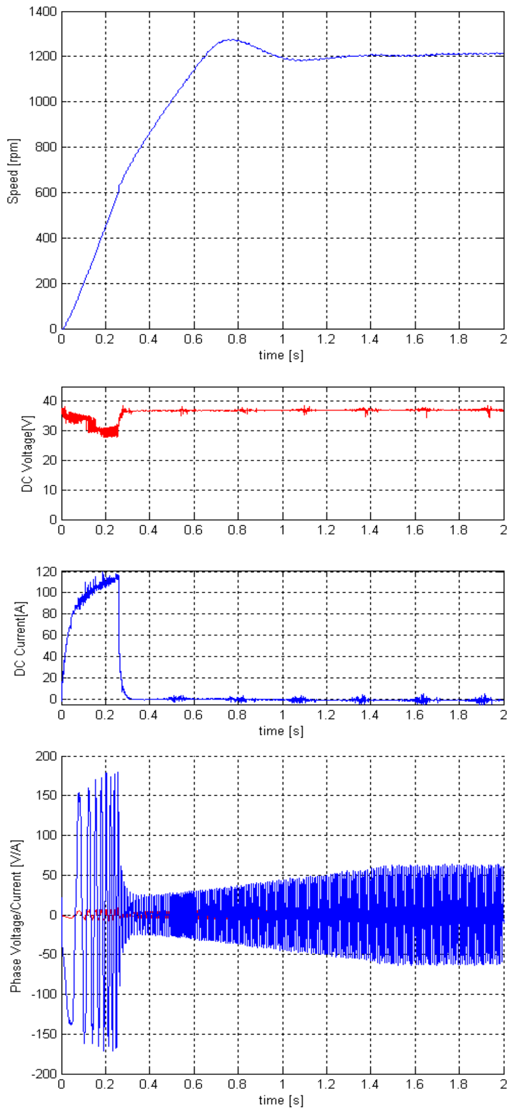

Fig.6 External characteristics of the ISG system

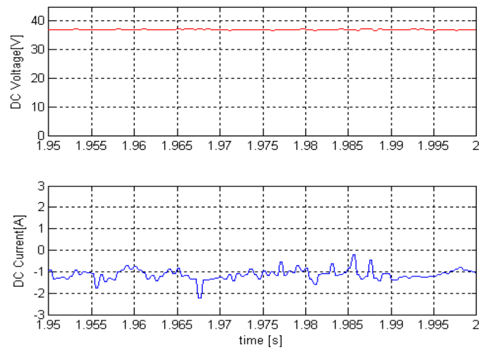

Fig.7 Expanded view of the DC outputs

its specific geometry and construction. For the generating regime, the phase voltage and current are presented in Fig.8. The current and voltage space phasor loci in the stationary reference frame presented in Fig.9 confirm the presence of the fifth harmonic in the phase current of the ISG [8]. These currents are acquired and used to generate the reference voltages commands and consequently these present many oscillations, as we can see in Fig.10a and 10b. In the absence of the corresponding transducer, Fig.10c shows the estimated generated electromagnetic torque by the ISG.

Once the start-up period was surpassed, the system will keep the engine-imposed speed and the same output voltage. While the battery pack is connected, this will keep the DC voltage approximately constant during non-high load variations.

The tested system presents good dynamic performances and responds well also in more complex situations.

5 Conclusion

This paper has provided a solution for an ISG by applying the vector control to an IPMSM. The proposed system is implemented both as a torque control scheme in motoring mode and as output voltage control scheme for the ISG driven by the variable speed engine.

A laboratory prototype for the ISG system has been implemented to validate the proposed method.

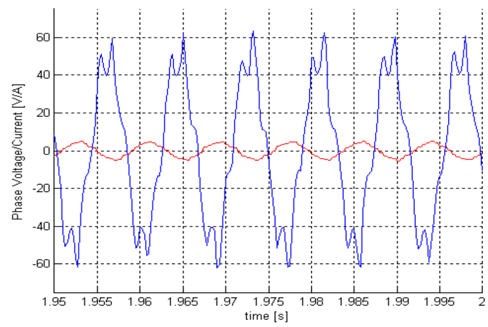

Fig.8 Expanded view of the ISG phase outputs

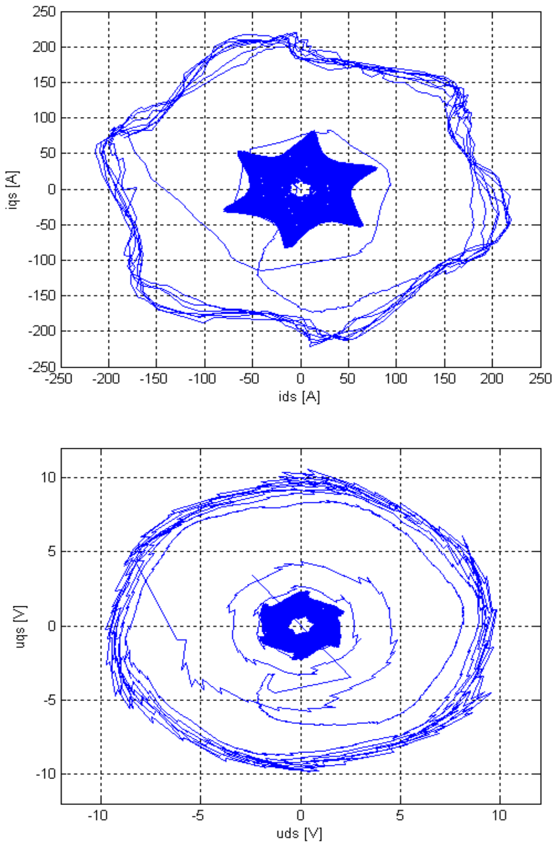

Fig.9 Current and voltage space phasor loci in the stationary reference frame

The results of the paper suggest that the controlled ISG responds to the specific demands in different operating conditions, offers good dynamic performances and represents an attractive ISG solution.

References:

[1] J. H. Song, J. M. Kim, and S. K. Sul, A new robust SPMSM control to parameter variations in flux weakening region, *IEEE IECON*, vol. 2, pp. 1193-1198, 1996.

[2] Y. S. Kim, Y. K. Choi and J. H. Lee, Speed-sensorless vector control for permanent-magnet synchronous motors based on instantaneous reactive power in the wide-speed region, *IEE Proc-Electr. Power Appl.*, vol. 152, No. 5, pp. 1343-1349, Sept. 2005.

[3] S. Morimoto, M. Sanada and K. Takeda, Wide-speed operation of interior permanent magnet synchronous motors with high performance current regulator, *IEEE Trans. Ind. Applicat.*, vol. 30, pp. 920-926, July/Aug. 1994.

[4] N.Bianchi, S.Bolognani, High-performance PM synchronous motor drive for an electrical scooter, *IEEE Trans. on Industry Applications*, vol.37, no.5, Sept./Oct.2001, pp.1348-1355

[5] C-T. Pan, S-M. Sue, A linear maximum per

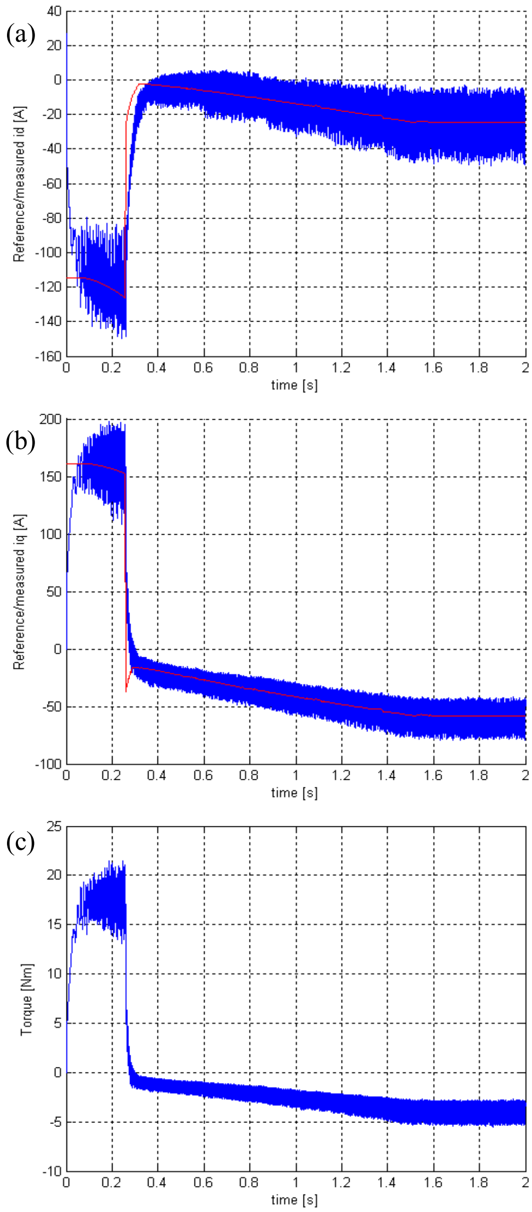

Fig.10 The reference and measured i_d , i_q currents and the estimated electromagnetic torque t_e

ampere control for IPMSM drives over full-speed range, *IEEE Trans. on Energy Conv.,* Vol.20, No.2, June 2005, pp.359-366

[6] J.L.Shi, T.H.Liu, S.H.Yang, Nonlinear controller design for an interior permanent-magnet synchronous motor including field weakening operation, *IET Electr. Power Appl.*, Vol.1, No.1. January 2007, pp. 119-126

[7] J. M. Kim and S. K. Sul, "Speed control of interior permanent magnet synchronous motor drive for the flux weakening operation," *IEEE Trans. Ind. Applicat.*, vol. 33, pp. 43-48, Jan./Feb. 1997.

[8] P. Vas, *Parameter Estimation, Condition Monitoring, and Diagnosis of Electrical Machines*, Clarendon Press, Oxford, 1993